IOSR Journal of Engineering (IOSRJEN) **www.iosrjen.org**
ISSN (e): 2250-3021, ISSN (p): 2278-8719
Vol. 08, Issue 01 (January. 2018), ||V1|| PP 75-84

Theoretical Calculation of Thermodynamic Properties of Refractory Metals Using A Semi-Emperical Interatomic Potential

Gbenga S. Agunbiade[1],Fadeke Matthew- Ojelabi[2],Nnaemeka C. Ogbu[3]
Taiwo H. Akande[4]
[1,2,4]*Computational and Condensed Matter Physics Group, Department of Physics, Ekiti State University, Ado Ekiti, Ekiti State. Nigeria*
[3]*Department of Physics, University of Ibadan, Ibadan, Oyo State. Nigeria*
Corresponding Author: Gbenga S. Agunbiade[1]

Abstract: *In this work, we have successfully applied one of the most effective semi - empirical interatomic potentials called embedded atom method EAM to calculate some thermodynamics properties of refractory metals (Nb, Ta, Mo and W). Our theoretical calculated values for mono-vacancy formation energy are in excellent agreement with the available experimental values. Among these metals, the highest* E_{1v}^{f} *is obtained for W. It is well known that the value of the mono-vacancy formation energy of each metal is directly proportional to its cohesive energy. i.e. the lower the cohesive energy is, the lower the mono-vacancy formation energy and vice versa. The trend exhibited by these metals whose mono-vacancy migration energies were computed revealed that migration energies are small but cannot be negative. The mono-vacancy activation energy was obtained by summing the mono-vacancy formation energy and mono-vacancy migration energy together. For all the metals considered, W has the largest values for mono-vacancy formation energy, mono-vacancy migration energy and mono-vacancy activation energy followed by Mo and then Ta. This could be as a result of parameter β used in the calculation. We used 8 as β for both W and Mo, while β = 6 for all other metals. The values for di-vacancy formation energy are larger than their corresponding mono-vacancy formation energy but still lower than corresponding cohesive energy of each metal. The binding energies were computed from mono-vacancy formation and di – vacancy formation energies. The obtained values for Nb and Ta metals are in good agreement with Zhang et al but there are no experimental values for these two metals. Experimental values are highly needed before conclusion can be drawn.*

Date of Submission: 05-01-2018 Date of acceptance: 20-01-2018

I. INTRODUCTION

The resistance against deformation at high temperatures makes the refractory metals suitable against strong forces at high temperature, for example in jet engines, or tools used during forging. Refractory metals are used in lighting, tools, lubricants, nuclear reaction control rods, as catalysts, and for their chemical or electrical properties. It is good to have fundamental knowledge of structure and thermodynamics properties of these metals in order to optimise their uses. To accomplish this, atomistic simulation would be one of the most useful approaches to study these materials and obtain such knowledge. The size, the computational speed and accuracy of a potential must be taken into consideration while designing a good potential. The system size and computational speed are very important for modelling properties of materials especially the equilibrium properties. Another major factor that must be considered is the accuracy of the model. The model is expected to reproduce the properties of these materials as closely as possible. The computational speed is very important in materials science while high accuracy is germane in computational chemistry.

The quality of any good interatomic potential is highly determined by the properties predicted during simulation. Among all these potentials, embedded atom method EAM which was developed by Daw and Baskes (1983) has the ability to predict considerable quality of the properties of metals and alloys. If a researcher is interested in high accuracy, first-principles results are good to be used, one can use either density functional theory or quantum-chemical method but these methods can only be applied to systems containing at most hundred atoms and they are much more expensive. Unlike first principle approaches, EAM cam be used in simulation of systems containing millions atoms in just nanoseconds.

The EAM was firstly formulated by Daw and Baskes (1983) to study and obtain different properties of materials. Oh and Johnson (1989) developed EAM potentials for fcc, bcc and hcp, this was called analytic embedded atom method. A model for vanadium bcc metal using the Morse potential as the pair potential between atoms was presented by Foiles (1990). The model was used study various thermodynamic properties of

V. Wang and Boercker (1995) presented a potential for bcc metals. This potential was employed to obtain many anomalies displayed in the phonon spectra of bcc transition metals. Also, Zhang *et al.* (1999) formulated another version of EAM potential called simple analytic EAM for some bcc metals and this was used to predict thermodynamic properties of binary alloys of these metals. Huiqiu *et al.* (2004) added a modified term *M(P)* to the total energy of Johnson's analytic EAM model and the called it the modified analytic EAM (MAEAM) potential. The surface segregation and composition depth profiles of Al–Mg alloy were studied with Monte Carlo simulation and the MAEAM. Ahmad *et al.* (2004) and Akhter *et al.* (2005) used EAM potentials to present the thermal properties of noble metals Ag and Au which are in good agreement with the experimental results.

Based on the pair-potential formulation of Wang and Boercker (1995) and analytic embedding energy of Johnson and Oh (1989), Wilson and Riffe (2012) developed a normalized EAM model, which reasonably predicted bulk vibrational properties associated with all alkali metals. They also applied the model to study the surface of Na (110), they identified surface localized modes and calculated directionally resolved Debye temperatures for near-surface planes of atoms. We employed the embedded-atom method and the tight binding second moment approximation model of cohesion to determine the models parameters (EAM and TB-SMA parameters) for Ta, Mo and W metals and their solid state electron densities were also determined (Matthew-Ojelabi et al, 2017). These model parameters and electron densities with and without adjustment were used to determine dilute-limit heats of solution (unrelaxed and relaxed) of the binary alloys of Ta, Mo and W. The result we obtained shows how electron densities play a vital role in determining some of the properties associated with alloys and defects in metals.

Similarly, we extended the modified analytical embedded atom method, MAEAM to the study of interatomic potentials for body centred cubic (bcc) transition metals (Popoola et al, 2017). Some thermodynamic properties of these metals were calculated. The mono-vacancy formation energy neither increases nor decreases as the lattice constant increases. Their computed value for mono-vacancy migration energy is lower than the result of ab initio calculation. They suggested that this could be due to the discrepancy in the modification term, fitting parameter and the contribution to the energy from many-body effects in the embedding function. Their computed value of mono-vacancy activation energy is lower at most point compare to some other result of ab initio calculation. Recently, Agunbiade et al (2017) applied EAM model to three alkali metals Na, K and Cs. We firstly determined the model parameters and electron densities which were later used to calculate some thermodynamics properties of these metals and their binary alloys. The values we obtained for the heats of solution of their binary alloys are in good agreement with the available experimental values. We reported that the values for heats of solution of these alloys are all positive indicating negligible solubility.

In this work, the embedded atom method EAM is extended to theoretically study and calculate some thermodynamic properties of refractory metals. The metals used in this study were chosen based on the availability of experimental data, their industrial and technological applications, and availability of some physical constants of metals that are required for computation.

II. THEORY

The total energy E_{tot} of EAM model is divided into two distinct parts and it is written as

$$E_{tot} = \frac{1}{2}\sum_{i \neq j}\phi(r_{ij}) + F(\rho_i) \quad (1)$$

E_{tot} is the total internal energy of the system.

$\phi(r_{ij})$ is the two-body potential (pairwise) interaction between atom *i* and atom *j* whose separation is given by r_{ij}.

While $F(\rho_i)$ is the embedding energy of atom *i* with the host electron density ρ_i at atom *i* due to all its surrounding atoms. And it is a measure of the atomic density in the neighbourhood of atom *i* that requires $f(r_{ij})$ to be a monotonically decreasing function of r_{ij}.

The background electron density ρ_i which will locally be determined for each particle and approximated as the sum of electron contributions from nearby particle is given by

$$\rho_i = \sum_{i \neq j} f(r_{ij}) \quad (2)$$

$f(r_{ij})$ is the atomic electron density at atom *i* due to atom *j* as a function of the distance between them.

The functional forms of $f(r)$ and $\phi(r)$ are taken and fit to experimental data while $F(\rho)$ is strictly derived from universal equation of state for bcc metals.

Firstly, the atomic electron density function $f(r)$ is given by

$$f(r) = f_e \exp\left[-\beta\left(\frac{r}{r_{1e}} - 1\right)\right] \quad (3)$$

As expected, the electron density is expected to be directly proportional to the cohesive energy and inversely proportional to the atomic volume of the metals.

As a result of this, the parameter f_e according to Johnson (1989) is taken as

$$f_e = \frac{SE_c}{\Omega} \quad (4)$$

S = 1 for all pure metals, E_C is the cohesive energy and Ω is the atomic volume for pure elements.

Secondly, the two-body (pairwise) potential $\phi(r)$ for this work which is the modified form of Rose *et al* (1984) can be expressed as

$$\phi(r) = -\phi_e\left[1 + \xi\left(\frac{r}{r_{1e}} - 1\right)\right] \times \exp\left[-\gamma\left(\frac{r}{r_{1e}} - 1\right)\right] \quad (5)$$

r_{1e} is the first equilibrium nearest neighbour distance. ϕ_e, ξ and γ are the adjustable model parameters that will later be determined.

Combining equation (1) and (2) for monoatomic metallic perfect crystal of bcc and considering the first equilibrium neighbour distance (r_{1e}) and the second neighbour distance (r_{2e}), we have

$$E(r) = F(\rho) + 4(r_{1e}) + 3(r_{2e}) \quad (6)$$

$$\rho(r) = 8f(r_{1e}) + 6f(r_{2e}) \quad (7)$$

Where $r_{2e} = Zr_{1e}$ and $Z = \frac{2}{\sqrt{3}}$ (8)

An exponentially decay electron density ρ is assumed to be

$$\rho(r_1) = \rho_e \exp\left[-\beta\left(\frac{r}{r_{1e}} - 1\right)\right] \quad (9)$$

The equilibrium electron density ρ_e is obtained by combining equation (4.3) & (4.9) at $r = r_{1e}$, and is given as

$$\rho_e = 8f_e + 6f_e \exp[-\beta(Z-1)] \quad (10)$$

According to Rose et al (1984)

$$E(r) = -E_c\left[1 + \alpha\left(\frac{r}{r_{1e}} - 1\right)\right] \times \exp\left[-\alpha\left(\frac{r}{r_{1e}} - 1\right)\right] \quad (11)$$

Where $\alpha = \sqrt{\frac{9\Omega B}{E_c}}$ (4.12)

B is the bulk modulus, Ω is the atomic volume and E_c is the cohesive energy of pure bcc metals.

By combining equation (6) and (11) to have

$$F(r) = -E_c\left[1 + \alpha\left(\frac{r}{r_{1e}} - 1\right)\right] \times \exp\left[-\alpha\left(\frac{r}{r_{1e}} - 1\right)\right] - 4\phi(r_{1e}) - 3\phi(r_{2e}) \quad (13)$$

By substituting $-\frac{1}{\beta}\ln\left(\frac{\rho}{\rho_e}\right)$ for $\left(\frac{r}{r_{1e}}-1\right)$ in equations (5) and (13) we obtain

$$\begin{aligned} F(\rho) \;=\; & -E_c\left[1-\frac{\alpha}{\beta}\ln\left(\frac{\rho}{\rho_e}\right)\right]\left(\frac{\rho}{\rho_e}\right)^{\alpha/\beta} - 4\phi_e\left[1-\frac{\xi}{\beta}\ln\left(\frac{\rho}{\rho_e}\right)\right]\left(\frac{\rho}{\rho_e}\right)^{\gamma/\beta} \\ & - 3\phi_e\left[1-\frac{Z\xi}{\beta}\ln\left(\frac{\rho}{\rho_e}\right)+\zeta(Z-1)\right]\left(\frac{\rho}{\rho_e}\right)^{Z\gamma/\beta}\times\exp\left[-\gamma(Z-1)\right] \end{aligned} \tag{14}$$

Apparently, the $F(\rho)$ presented in our present work is very simple with just three undetermined parameters. These model parameters (ξ , γ and ϕ_e) can be determined with the following equations

$$4r_{1e}\,\phi'(r_{1e}) + 3r_{2e}\,\phi'(r_{2e}) = 0 \tag{15}$$

$$4r_{1e}^2\,\phi''(r_{1e}) + 3r_{1e}^2\,\phi''(r_{2e}) = 15\Omega G \tag{16}$$

$$E_{1f} = -4\phi(r_{1e}) - 3\phi(r_{2e}) + \frac{1}{2}F''(\rho_e)\left[8f^2(r_{1e}) + 6f^2(r_{2e})\right] \tag{17}$$

Substituting the expressions for $f(r)$, $\phi(r)$ and $F(\rho)$ respectively from equations (3), (5) and (14) into equation (15) to (17) and considering their differentiations to yield

$$4(\gamma-\beta) + 3Z\left[\gamma-\xi+\gamma\xi(Z-1)\right]\times\exp\left[-\gamma(Z-1)\right] = 0 \tag{18}$$

$$4\phi_e\gamma\left\{\gamma-2\xi + \left[\gamma-2\xi + \gamma\xi(Z-1)\right]\times\exp\left[-\gamma(Z-1)\right]\right\} = 15\Omega G \tag{19}$$

$$E_{1f} = -4\phi_e - 3\phi_e\left[1+\xi(Z-1)\right]\times\exp\left[-\gamma(Z-1)\right] + (9\Omega B - 15\Omega G)\frac{8+6\exp\left[-2\beta(Z-1)\right]}{2\beta^2\left\{8+6\exp\left[-2\beta(Z-1)\right]\right\}^2} \tag{20}$$

So far, all the model parameters for this work f_e, ϕ_e, α , β , γ and ξ can be determined using the physical input parameters cohesive energy, unrelaxed mono-vacancy formation energy, lattice constant and elastic constants ($C_{11,}$ C_{12} and C_{44}) from which bulk modulus and Voigt average shear modulus are determined. With these model parameters, we now have a complete EAM model. The physical input parameters which are taken from different literatures are presented in table 1

While all the EAM model parameters for this work (f_e, ϕ_e, α , β , γ and ξ) are presented in table 2

2.1Energy Calculations

Mono-vacancy is formed by removing one atom from the central site of a crystal with N atoms and the formation energy of mono-vacancy E_{1v}^f can be calculated by

$$E_{1v}^f = E_{tot}^{N-1} - \frac{(N-1)}{N}E_{tot}^N \tag{21}$$

E_{tot}^{N-1} is the total energy of the crystal with mono-vacancy

E_{tot}^N is the total energy of the perfect crystal without mono-vacancy

The mono-vacancy migration energy be determined using the diffusion coefficient of mono-vacancy and is given as

$$D_{1v} = D_{1v}^0\exp\left[\frac{-E_{1v}^m}{k_BT}\right] \tag{22}$$

D_{1v} is the diffusion coefficient of mono-vacancy, D_{1v}^0 is the pre-exponential factor, E_{1v}^m is the mono-vacancy migration energy, k_B is the Boltzman's constant and T is the temperature.

The mono-vacancy activation can be calculated from by summing both mono-vacancy formation and mono-vacancy migration energies

$$Q_{1v} = E_{1v}^{f} + E_{1v}^{m} \quad (23)$$

Similarly, the di-vacancy formation energy is possible and this can equally be calculated by removing two atoms from a perfect crystal of each bcc metals which is given by

$$E_{2v}^{f} = E_{tot}^{N-2} - \frac{(N-2)}{N} E_{tot}^{N} \quad (24)$$

E_{tot}^{N-2} is the total energy of the crystal with di-vacancy

E_{tot}^{N} is the total energy of the perfect crystal without di-vacancy

Another form of energy that can be calculated with this present model is the binding energy of di-vacancy. The binding energy is the difference between the mono-vacancy and di-vacancy formation energies. This is given as

$$E_{2b} = 2E_{1v}^{f} - E_{2v}^{f} \quad (25)$$

The input physical parameters for refractory metals considered in this work are presented in table 1. The lattice constant a_0 is in Å, atomic volume Ω is in Å^3, cohesive E_c & vacancy formation E_{1v} energies are in eV, while C_{11}, C_{12}, C_{44}, B and G are in eV/Å^3.

Table 1: The Input Experimental Parameters for BCC Transition Metals

	a_0 [a]	E_c [b]	E_{1v} [c, d]	C_{11} [d,e,f]	C_{12} [d,e,f]	C_{44} [d,e,f]	Ω	B	G
Nb	3.3008	7.47	2.75	1.531	0.825	0.176	17.9816	1.0603	0.2470
Ta	3.3026	8.10	2.95	1.650	0.988	0.516	18.0110	1.2087	0.4420
Mo	3.1469	6.82	3.10	2.869	1.050	0.694	15.5818	1.6563	0.7800
W	3.1650	8.66	3.95	3.231	1.269	0.981	15.8523	1.9230	0.981

[a] West (1984) [b] Kittle (1976) [c] Puska and Nieminen (1997)
[d] Hearmon (1983) [e] Simmons and Wang (1991) [f] Mishra and Singh (1990).

III. RESULTS AND DISCUSSION

3.1results

This section will be presenting all the results obtained in this research work. While using EAM, there are some model parameters that must be determined. So far, we have firstly determined all the model parameters for this work f_e, ϕ_e, α, β, γ and ξ (table 2) using the physical input parameters; cohesive energy, unrelaxed mono-vacancy formation energy, lattice constant and elastic constants (C_{11}, C_{12} and C_{44}) from which bulk modulus and Voigt average shear modulus are determined.

Table 2: The calculated EAM model parameters for refractory metals

	f_e	ϕ_e	ξ	α	γ	β
Nb	0.4154	0.3877	6.1611	4.7928	4.8195	6
Ta	0.4497	0.4342	8.1665	4.9182	6.2097	6
Mo	0.4376	0.4458	10.4527	5.8358	7.8558	8
W	0.5463	0.6232	10.0431	5.6286	7.5551	8

Table 3: Mono-Vacancy Formation Energy E_{1v}^{f} for refractory metals

	Present model	Exp. Data [a]	EAM of Johnson [b]	FS model [c]
Nb	2.71	2.7	2.95	2.48
Ta	2.93	3.1	2.95	2.87
Mo	3.05	3.2	3.20	2.54
W	3.95	3.6	3.95	3.62

Table 4: Mono-Vacancy Migration Energy E_{1v}^{m} for refractory metals

	Present model	Exp. Data [a]	EAM of Johnson [b]	FS model [c]
Nb	0.83	0.55	0.97	0.91
Ta	0.78	0.70	1.15	1.22

Mo	1.41	1.35	1.62	1.32
W	1.56	1.70	1.97	1.49

Table 5: Mono-Vacancy Activation Energy Q_{1v} for refractory metals

	Present model	Exp. Data [a]	EAM of Johnson [b]	FS model [c]
Nb	3.54	3.7	3.85	3.39
Ta	3.71	3.8	3.91	4.09
Mo	4.46	4.5 [d]	4.54	3.86
W	5.51	5.4	5.54	5.11

[a] – Siegel et al. (1982) [b] – Guellil and Adams (1992)
[c] – Harder and Bacon (1986) [d] – Marier et al. (1979)

Table 6: Di-Vacancy Formation Energy E_{2v}^{f} for refractory metals

	Present model	Exp. Data	Zhang *et al* (1999)
Nb	5.13	-	5.107
Ta	5.51	-	5.466
Mo	5.69	-	5.75
W	7.45	-	7.32

Table 7: Di-Vacancy Binding Energy E_{2v}^{b} for refractory metals

	Present model	Exp. Data Musada (1982)	Zhang *et al* (1999)
Nb	0.29	-	0.393
Ta	0.35	-	0.434
Mo	0.41	0.393	0.450
W	0.45	0.451	0.580

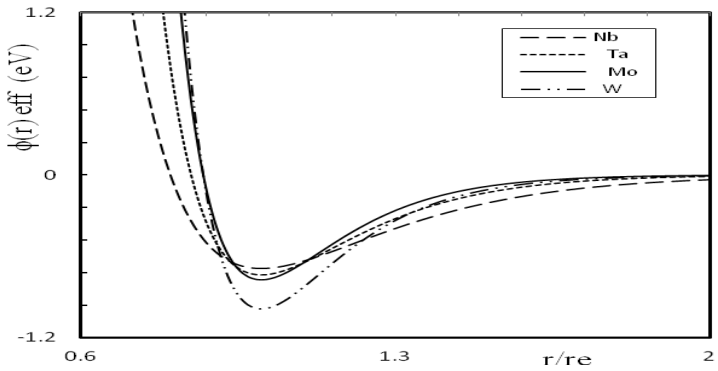

Figure 1 : The variation of two – body potential with relative distance for refractory metals

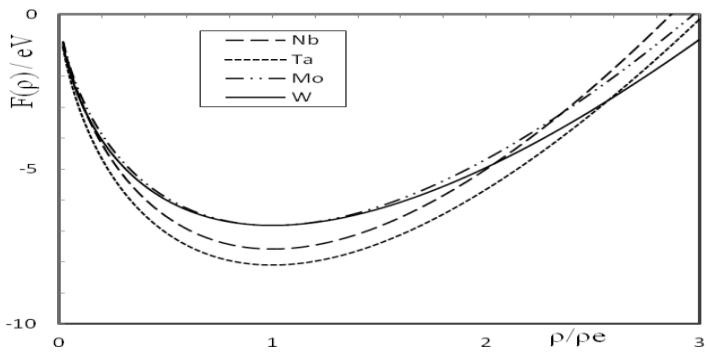

Figure 2 : The variation of emdedding function with relative denstiy for refractory metals

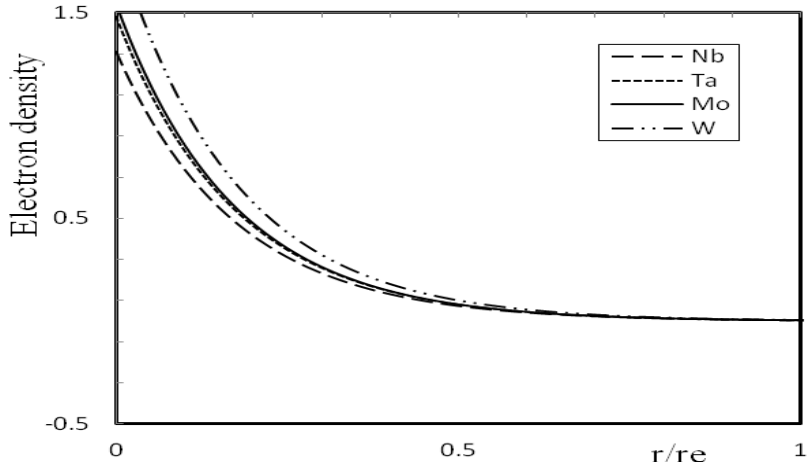

Figure 3 : The variation of atomic electron density with relative distance for refractory metals

3.2DISCUSION

3.2.1Mono-Vacancy Formation Energy E_{1v}^{f}

The formation energy of a vacancy reflects the bond strength of the solid. To calculate the mono-vacancy formation energy, some steps are necessary to be taken. Firstly, there must be a perfect crystal, then remove an atom, later relax the system, now evaluate the potential energy and finally calculate the vacancy formation energy using equation (21) or equation (17) of EAM model described in the previous section. The mono-vacancy formation energies, E_{1v}^{f} for refractory metals are presented in table 3 together with the available experimental data and values obtained by other authors. It can be clearly seen from the two tables that our theoretical calculated values are in excellent agreement with the available experimental values. Among these metals, the highest E_{1v}^{f} is obtained for W. It is well known that the value of the mono-vacancy formation energy of each metal is directly proportional to its cohesive energy. i.e. the lower the cohesive energy is, the lower the mono-vacancy formation energy and vice versa. (Popoola et al., 2017) have previously calculated the mono-vacancy formation energies for bcc transition metals using modified analytical embedded atom method (MAEAM). Though, the results they obtained were in good agreement with the experimental data but the modification they used in MAEAM added a complexity to their calculation. The current EAM model used for this work is simple with no complexity.

The vacancy formation energy value we obtained for Ta metal is 2.93eV and this values is smaller by 5.48% than the experimental value which is 3.1eV. Also, for Mo metal, we obtained 3.05eV which is as well smaller by 4.69% than the available experimental data for Mo (3.2eV). But for W metal, our calculated value which is 3.95eV is higher by 9.7% than experimental value (3.6eV). The difference in each metal could be as a result of structural relaxation associated with vacancy formation energy.

Also, our present calculated values are closer to experimental values than the values from other authors. For Ta and W metals, FS model also predicted lower values to experimental values, our calculated values for these two metals (Ta and W) are better than values from FS model. With these, we can say our obtained values are in excellent agreement with available experiment values.

3.2.2Mono-Vacancy Migration Energy E_{1v}^{m}

Migration energy for vacancy is the difference between the energy for saddle point and that of equilibrium site (Wangyu et al., 2002). According to vacancy mechanism for diffusion, an atom overcomes a potential barrier when it migrates from its original site to the vacancy site. The maximum point for the potential barrier (saddle point) is located at the mid-point of the migration path. Our theoretical calculated values for mono-vacancy migration energies for refractory metals are listed in table4. The available experimental data together with values obtained by different authors are also presented. The trend exhibited by these metals in table 4 whose mono-vacancy migration energies are computed revealed that migration energies are small but cannot be negative. The values predicted by Guellil and Adams (1992) using EAM model developed by Johnson are higher than the FS model used by Torrem and Gerl (1969). The present calculations are closer to the experimental values better than Guellil and Adams and even Torrem and Gerl calculations. It also good to know that the actual experimental values for E_{1v}^{m} are difficult to find. The values listed for experimental migration

energy are just calculations made by subtracting the experimental values of mono-vacancy formation energy from mono-vacancy activation energy.

3.2.3Mono-Vacancy Activation Energy Q_{1v}

The mono-vacancy activation energy is the sum of mono-vacancy formation energy and mono-vacancy migration energy (equation 23). Our present calculations for mono-vacancy activation energy for refractory metals are shown in table 5. For better comparison, the available experimental data together with values from previous authors are also presented. For all metals considered in this work, W has the largest values for mono-vacancy formation energy, mono-vacancy migration energy and mono-vacancy activation energy followed by Mo and then Ta. This could be as a result of parameter β used in the calculation. We used β = 8 for both W and Mo, while β = 6 for all other metals. It could be as a result of W, Mo and Ta belonging to members of refractory metals.

3.2.4 Di-vacancy Formation Energy E_{2v}^{f}

Di-vacancy formation energy is computed by similar method used in mono-vacancy formation energy. The only difference between them is the number of atom(s) removed from their perfect crystals. A single atom is needed to be removed in a perfect crystal to compute its mono-vacancy formation energy while two atoms must be removed to create vacancies in di-vacancy. Using equation (4.24), the di-vacancy formation energies are computed and listed in table 6 for these metals. The available experimental data are also listed. Two configurations are only considered, which are; the first-nearest-neighbour (nn) and the second-nearest-neighbour (nnn) di-vacancy. According to Zhang et al. (1994), for di-vacancy diffusion in bcc metals, the di-vacancy must migrate either by a one-step next-nearest neighbour (nnn) jump to the nearest-neighbour divacancy or by a two-step jump, first to an intermediate metastable configuration and then to form a nearest-neighbour (nn) di-vacancy.

During computation, there is little or no difference for each metal configuration between the first-nearest-neighbour and second-nearest-neighbour, so just a single configuration is considered in this work.
Finally, it is good to know that the values for di-vacancy formation energy are larger than their corresponding mono-vacancy formation energy but still lower than corresponding cohesive energy of each metal.

3.2.5Di-vacancy Binding Energy E_{2v}^{b}

The binding energies computed from mono-vacancy formation and di – vacancy formation energies using equation (25) are shown in table 7 for these metals. The obtained values for Nb and Ta metals are in good agreement with Zhang et al (1999) but there are no experimental values for these two metals. Experimental values are highly needed before conclusion can be drawn. The obtained values for Mo and W with the present model are in excellent agreement with the experimental values better than Zhang et al (1999).
As observed for mono- vacancy and di-vacancy energise, W still have the highest values for the binding energy among these refractory metals.

3.2.6The Two-body Potential Graph

The two-body potentials for all the refractory metals (Nb, Ta, Mo and W) are shown in figure 5.1, it could be observed that the pair-potential function displaced steep repulsion interactions at short distances. While at large distances, weak attractions are observed and shallow wells at intermediate distances for all metals. The metals are expected to display some similar properties. W has the lowest distinct minimum curve among these metals, followed by Mo, then Ta and Nb in that order. The lowest minimum curve exhibited by W could be attributed to its thermal properties (highest melting and boiling points).

3.2.7The Embedding Function Graph

Figure 2 presents the embedding function graphs for refractory metals (Nb, Ta, Mo and W) The embedding functions can be seen to be slightly deviated from symmetrical parabolic function. It should be noted that there is an invariant transformation of EAM and because of this, any simultaneous transformation of ρ and $F(\rho)$ functions would not affect the overall embedding energies. Figure 2 follows the same trend for all the metals. The minimum curves for Mo and W overlap with Ta having the lowest minimum curve.

3.2.8The Electron Density graph

The variations of electron density with relative distance are in figure 3. As expected, the electron density decreases as the relative distance increases with the distinct atoms contributed little to the background electron density on the centre atom. The electron density displayed a very low background electron density at

large distances, the background electron density increased sharply as the distances approach to the first coordination layer. With this, we can easily say that the background electron density was mainly contributed by atoms in the first coordination layer. All the metals here follow same the trend. As their electron densities approach zero, they all converge and follow a straight line even with further increase in relative distance, they all still follow this straight line.

III. CONCLUSION

In this research work, we have successfully applied one of the most effective semi - empirical interatomic potentials called embedded atom method to study some properties of refractory metals (Nb, Ta, Mo and W). The ability of these refractory metals to withstand high temperature makes them very useful in different applications. Our theoretical calculated values for mono-vacancy formation energy are in excellent agreement with the available experimental values. Among these metals, the highest E_{1v}^{f} is obtained for W. It is well known that the value of the mono-vacancy formation energy of each metal is directly proportional to its cohesive energy. i.e. the lower the cohesive energy is, the lower the mono-vacancy formation energy and vice versa.

We also obtained the mono-vacancy migration energies for these metals. The trend exhibited by these metals whose mono-vacancy migration energies are computed revealed that migration energies are small but cannot be negative. It is good to note that the values listed for experimental migration energy are just calculations made by subtracting the experimental values of mono-vacancy formation energy from mono-vacancy activation energy. The mono-vacancy activation energy was also considered. This was obtained by summing the mono-vacancy formation energy and mono-vacancy migration energy together. For all metals considered in this work, W has the largest values for mono-vacancy formation energy, mono-vacancy migration energy and mono-vacancy activation energy followed by Mo and then Ta. This could be as a result of parameter β used in the calculation. We used β = 8 for both W and Mo, while β = 6 for all other metals. It could also be as a result of W, Mo and Ta belonging to members of refractory metals.

Finally, the di-vacancy formation energy is computed by similar method used in mono-vacancy formation energy. The only difference between them is the number of atom(s) removed from their perfect crystals. The values for di-vacancy formation energy are larger than their corresponding mono-vacancy formation energy but still lower than corresponding cohesive energy of each metal. The binding energies are as well computed from mono-vacancy formation and di – vacancy formation. The obtained values for Nb and Ta metals are in good agreement with Zhang et al (1999) but there are no experimental values for these two metals. Experimental values are highly needed before conclusion can be drawn.

REFERENCES

[1]. Agunbiade G. S, Akande T. H. and Matthew-Ojelabi F. Modelling of Na, K & Cs Alkali Metals and their Binary Alloys Using a Simple Analytical Embedded Atom Method (EAM). Accepted for publication: IOSR-JAP, (2017) India, **.**

[2]. Ahmad E., Akhter J. I. and Ahmad M. Computational Material Science, **31**; (2004) 309.

[3]. Akhter J. I., Yaldram K. and Ahmad W. Solid status comm. 98 (1996) p1043.

[4]. Daw M. S. and Baskes M. I. Semiemperical, Quantum Mechanical Calculation of Hydrogen Embrittlement in Metal. Phys. Rev. Lett. 50, (1983) 1285-1288.

[5]. Foiles M. I. Surface Segregation and Related Phenomena edited by P.A. Dowben and Miller, A. (CRC, Boca Raton) Vol. 1 (1990) P.79.

[6]. Guellil A. M. and Adams J. B. The Application of Analytical Embedded Atom Method to bcc Metals and Alloys. J. Matter Res. 7 (1993), 639.

[7]. Harder J. M. and Bacon D. J. Point-defect and stacking-fault properties in bcc metals with N-body interatomic potentials. Philos. Mag. A, 54 (1986) 651–661.

[8]. Hearmon R. F. S. Landolt-Bornstein, New series, Vol. III/1, 1966; Vol. III/2, 1978; Vol. III/18, (1986) Springer-Verlag, Heidelberg.

[9]. Huiqiu Deng, Wangyu Hu, Xiaolin Shu, Bangwei Zhang. Analytic embedded-atom method approach to studying the surface segregation of Al–Mg alloys. Applied Surface Science 221, (2004) 408–414

[10]. Johnson R. A. and Oh D. J. Analytical embedded atom method model for bcc metals. J. Mater. Res. 4, (1989) 119.

[11]. Kittle C. Introduction to Solid Physics 5th edition (1976) ,New York: Wiley p74.

[12]. Marier K., Mehrer H. and Rein G., 1979. MetalikdeI 70.

[13]. Matthew-Ojelabi F., Agunbiade G. S. and Akande T. H. Atomistic Simulations of Ta, Mo & W and Their Binary Alloys Using Embedded Atom Method and Second Moment Approximation of Tight Binding, Int. J. of Inn. Res. & Adv. Studies (IJIRAS), Vol. 4 (2), (2017) 400-404.

[14]. Mishra S.K. and Singh T.N. Phys. Stat. Sol. (b) 158, (1990) 153

[15]. Popoola O. O., Matthew-Ojelabi F., Agunbiade G. S., Adesakin G. E. & Akande T. H. Modified Analytical Embedded Atom Method (MAEAM) Interatomic Potentials for Body Centred Cubic (BCC) Transition Metals And Vacancy Mechanism, Int. J. of Sci. Res. (IJSR), Vol. 6 (4) , (2017) 670-673.
[16]. Siegel R.W., Doyama M. and Kiritari M. Proceedings of Yamada conference on point Defects and Defects interactions in metals, university of Tokyo press, (1982) Tokyo, P. 533
[17]. Simmons R.O. and Wang H. Single Crystal Elastic Constants and Calculated Aggregate Properties: A Handbook (MIT Press, Cambridge, MA,) (1991)
[18]. Wang Y. R. and Boercker D. B. Journal of Applied Physics 78, (1995) 122.
[19]. West A.R., Solid State Chemistry and its Applications. Wiley press, (1984). New York.
[20]. Wilson R. B. and Riffe D. M. An Embedded-Atom-Method Model for Alkali-Metal Vibrations. J. Phys. Condens. Matter **24**, (2012) 335401.
[21]. Zhang B., Ouyang Y., Liao S. and Jin Z. Physical B.262 (1992) p.281.

Gbenga S. Agunbiade. "Theoretical Calculation of Thermodynamic Properties of Refractory Metals Using A Semi-Emperical Interatomic Potential." IOSR Journal of Engineering (IOSRJEN), vol. 08, no. 01, 2018, pp. 75–84.